

**MAPPING SURFACE FUELS USING LIDAR AND
MULTISPECTRAL DATA FUSION FOR FIRE BEHAVIOR
MODELING**

A Thesis

by

MUGE MUTLU

Submitted to the Office of Graduate Studies of
Texas A&M University
in partial fulfillment of the requirements for the degree of

MASTER OF SCIENCE

December 2006

Major Subject: Forestry

**MAPPING SURFACE FUELS USING LIDAR AND
MULTISPECTRAL DATA FUSION FOR FIRE BEHAVIOR
MODELING**

A Thesis

by

MUGE MUTLU

Submitted to the Office of Graduate Studies of
Texas A&M University
in partial fulfillment of the requirements for the degree of

MASTER OF SCIENCE

Approved by:

Chair of Committee, Sorin C. Popescu

Committee Members, Marian Eriksson

Ross F. Nelson

Lewis Ntaimo

Head of Department, Steven Whisenant

December 2006

Major Subject: Forestry

ABSTRACT

Mapping Surface Fuels Using LIDAR and Multispectral Data Fusion for Fire Behavior Modeling. (December 2006)

Muge Mutlu, BAR, Cukurova University, Turkey

Chair of Advisory Committee: Dr. Sorin C. Popescu

Fires have become intense and more frequent in the United States. Improving the accuracy of mapping fuel models is essential for fuel management decisions and explicit fire behavior prediction for real-time support of suppression tactics and logistics decisions. This study has two main objectives. The first objective is to develop the use of Light Detection and Ranging (LIDAR) remote sensing to assess fuel models in East Texas accurately and effectively. More specific goals include: (1) developing LIDAR derived products and the methodology to use them for assessing fuel models; (2) investigating the use of several techniques for data fusion of LIDAR and multispectral imagery for assessing fuel models; (3) investigating the gain in fuels mapping accuracy with LIDAR as opposed to QuickBird imagery alone; and, (4) producing spatially explicit digital fuel maps. The second objective is to model fire behavior using FARSITE (Fire Area Simulator) and to investigate differences in modeling outputs using fuel model maps, which differ in accuracy, in east Texas.

Estimates of fuel models were compared with in situ data collected over 62 plots. Supervised image classification methods provided better accuracy (90.10%) with the fusion of airborne LIDAR data and QuickBird data than with QuickBird imagery alone

(76.52%). These two fuel model maps obtained from the first objective were used to see the differences in fire growth with fuel model maps of different accuracies. According to our results, LIDAR derived data provides accurate estimates of surface fuel parameters efficiently and accurately over extensive areas of forests. This study demonstrates the importance of using accurate maps of fuel models derived using new LIDAR remote sensing techniques.

DEDICATION

To my son, Arda Kaan and my dear husband, Atilla

*Thanks for your patience and constant
support of my work on my research*

ACKNOWLEDGEMENTS

First, thanks to God for everything that I have today.

I would like to express my sincere appreciation to Dr. Sorin C. Popescu, my committee chair and advisor, for giving me the opportunity to pursue my MS degree. I would not have been successful without his help. He provided the constant encouragement, advice, and motivation that I really needed in order to get this work done. His performance and original thought have pushed me to learn and grow more and more. Especially, I will never forget his support and understanding when I had my son, Arda Kaan. I really thank him from my heart.

I wish to thank all my committee including: Dr. Eriksson, Dr. Nelson, and Dr. Ntamo for all their advice, support, and patience.

I express my gratitude to the Spatial Science Lab, Department of Forest Science, and Texas A&M University for providing me with the assistance and invaluable resources to complete this degree. This study was funded by the Texas Forest Service (award # 02-DG-11083148-050). I would like to thank all Texas Forest Service personnel, especially Curt Stripling, Tom Spencer and Brad Smith, for all their help on collecting field data and determining fuel models based on these datasets.

Thanks also to all my friends for their help, encouragement, understanding, and love, especially Gokcen, my best friend, thanks for listening and supporting me when I needed to talk to somebody. Mandi, thank you for editing my writing. Kim, De Et'ra, Julie, Selma, Alicia, and Kaiguang, I am lucky to have you all as my friends.

From the depth of my heart, I would like to thank my husband, Atilla Mutlu for his unfailing love and sacrifice. He deserves all the credit for my graduation. He has been a constant source of support and encouragement, and very understanding when I needed to work long hours or change family plans to accommodate research objectives. I truly thank him for taking care of our baby when I was not around and understanding me. You are a perfect husband and daddy. I am indeed lucky to have found such a great partner. I must not forget to thank my son. Although he is only 4 months old, he has been very helpful too. Thank you, my little Arda Kaan, for sleeping well during the night and being a good boy when I have to work at home. You both are my everything and I love both of you so much.

I also would like to thank my parents, Tahsin and Sevinc Agca, my sister, Sule, my brothers, Bilgehan and Erhan, for their support and love. Even though they are back in Turkey, I always feel their love in my heart. They never let me feel alone.

TABLE OF CONTENTS

	Page
ABSTRACT	iii
DEDICATION	v
ACKNOWLEDGEMENTS.....	vi
TABLE OF CONTENTS	viii
LIST OF FIGURES.....	x
LIST OF TABLES	xii
 CHAPTER	
I INTRODUCTION	1
Objectives.....	5
Thesis Organization.....	5
II LITERATURE REVIEW	7
III MAPPING SURFACE FUEL MODELS USING LIDAR AND MULTISPECTRAL DATA FUSION.....	10
Introduction	10
Materials and Methods	12
Study Area.....	12
Data	13
LIDAR Data	13
Ground Inventory Data.....	15
Processing Approach.....	17
Height Bins Approach.....	18
Data Fusion Approach.....	20
LIDAR-derived Stack	21
Principal Component Analysis (PCA)	22
Minimum Noise Fraction (MNF)	24
Image Processing.....	26
Results and Discussion.....	27

CHAPTER	Page
IV USING LIDAR-DERIVED FUEL MAPS WITH FARSITE FOR FIRE BEHAVIOR MODELING	30
Introduction	30
Materials and Methods	31
Data	32
Dataset with LIDAR_derived Fuel Map	32
Dataset with QuickBird-derived Fuel Map	34
Fire Simulation	34
Processing Approach.....	35
Results and Discussion.....	37
V CONCLUSIONS	41
REFERENCES.....	44
VITA	50

LIST OF FIGURES

FIGURE	Page
3.1	Example of (a) grass fuel model, (b) brush fuel model, and (c) timber fuel model on the study area..... 11
3.2	Map of Texas indicating the location of our study area and false color composite of QuickBird image, with field plot locations 13
3.3	Flight lines over the Huntsville area 14
3.4	(a) Location of Plot #8 in the study area shown on the QuickBird image, (b) digital photos of Plot #8..... 16
3.5	The flowchart of processing approach 18
3.6	(a) The 3D of laser hits of Plot 9, (b) zoom in view of Plot 9, and (c) the digital photograph from the area..... 19
3.7	Overall view of the eleven Height Bins. (a) Bin 1: 0-0.5 m, (b) Bin 2: 0.5-1.0 m, (c) Bin 3: 1.0-1.5 m, (d) Bin 4: 1.5-2.0m, (e) Bin 5: 2.0-2.5 m, (f) Bin 6: 2.5-5.0 m, (g) Bin 7: 5.0-10.0 m, (h) Bin 8: 10.0-15.0 m, (i) Bin 9: 15.0-20.0 m, (j) Bin 10: 20.0-25.0 m, (k) Bin 11: >30.0 m..... 20
3.8	The LIDAR-QuickBird stack image 22
3.9	First five PC images 23
3.10	MNF images 25
3.11	(a) The classification result of multispectral QuickBird image, (b) the classification result of data fusion stack of LIDAR and Multispectral imagery, and (c) the classification result of PC stack image, (d) the classification result of MNF-fused stack image, and (e) legend for all classifications 28

FIGURE	Page
4.1 (a) The fuel map obtained by classifying a LIDAR and QuickBird fused data set, (b) the fuel model map obtained by classifying a QuickBird image	32
4.2 Screenshot from the fire simulation	35
4.3 Flow diagram illustrating the general procedure used to create the FARSITE inputs for both datasets	36
4.4 Comparison of burned areas for both fuel model maps	37
4.5 Comparison of fire perimeter results for both fuel model maps	38

LIST OF TABLES

TABLE	Page
3.1 Description of fuel models	17
3.2 Calculations of Eigenvalues, percentage of total variance and cumulative variance for each PC	24
3.3 Calculations of Eigenvalues, percentage of total variance and cumulative variance for each MNF	25
3.4 Comparison of results for all supervised image classifications	29
4.1 Fire fighting resource characteristics for LIDAR-derived fuel model map	40
4.2 Fire fighting resource characteristics for QuickBird-derived fuel model map	40

CHAPTER I

INTRODUCTION

Fire is a critical issue in many countries such as the United States, Southern Europe, Siberia, and Turkey (Falkowski et al., 2005) and fuel distribution is very important for defining fire behavior (Chuvieco and Congalton, 1989). Many forest fires occur each year and a huge amount of forest areas are lost in the US. For example, in Texas alone, in 2005 there were a total of 2,043 fires, which burned 51,675.12 hectares (127,692 acres). It has been reported by the Texas Forest Service (2006) that 8,015.2 hectares (19,806 acres) have burned in Texas already in the first five days of 2006. To mitigate fire risks, land managers should identify those areas most in need of fuel mitigation efforts. Managing such risk is difficult since fuel hazards are changing, and because fire behavior is affected by many factors, including weather, wind conditions, and topography. To improve ecosystem health, there is a need to use complex fire behavior models to support environmental assessments. Fire managers must provide more accurate fire behavior predictions, and there is a need to reflect on some factors such as canopy height, dead and live fuel load, and percent of canopy cover because these factors are known as fuel types (Pyne et al., 1996).

Fire managers usually group vegetation communities into fuel types based on similar potential fire behavior (Riano et al., 2002). In addition, fuel models can be used to describe fuels (Anderson, 1982). Fire managers usually group vegetation communities

This thesis follows the style of the journal, *Remote Sensing of Environment*.

into fuel types based on similar potential fire behavior (Riano et al., 2002). In addition, fuel models can be used to describe fuels (Anderson, 1982). Fuel type is an identifiable association of fuel elements of a distinctive plant species, form, size, arrangement, or other characteristics that will cause a predictable rate of fire spread or difficulty of control under specified weather conditions. Fuel model refers to a simulated fuel complex (or combination of vegetation types) for which all fuel descriptors required for the solution of a mathematical rate of spread model has been specified (Pyne et al., 1996).

Fire managers recognize a total of three general types of wildland fire according to the vegetation layer: ground, surface, and crown fire. The fire that grows in organic soils, roots, duff, wood, muck, peat and rotten buried is called ground fire (Scott, 2001) and this kind of fire grows really slow because roots, duff, muck, peat etc. burn slower than brush and grass vegetation types. A surface fire burns in the surface layer's dead and down limbs, forest needle and leaf litter, short trees, grass, and branch wood (Scott, 2001). A crown fire burns in the elevated canopy fuels. Canopy fuels normally consumed in crown fires consist of live and dead foliage. Assessing crown fire potential requires the most accurate estimates of canopy fuel characteristics possible (Scott, 2001). This study focused on surface fires.

Remote sensing can support many aspects of fire management and it can be used to decrease fire risk and to reduce fire damage. In recent years, remote sensing techniques have been applied to estimate fuel properties such as structure and density (Morsdorf, et. al., 2004; Pyne et al., 1996). Airborne LIDAR (Light Detection and

Ranging) systems have been used to estimate critical parameters for fire behavior and may, potentially, be used to compute and distinguish a range of fuel attributes including understory fuel height (Roff et al., 2005, and Means, 2000). Detailed information can be extracted from LIDAR remote sensing such as accurate geometric X, Y, and Z position of scattering elements which includes measurements of the forest canopy and ground surface (Lefsky et al., 2002). Airborne LIDAR remote sensing is a powerful tool to obtain fuel information. Compared to traditional aerial photography or fieldwork, airborne scanning laser systems provide better spatial coverage and enough temporal resolution to update fuel maps (Riano et al., 2003).

The use of airborne LIDAR allows scientists to measure the three-dimensional structure of the canopy, and it also allows for more accurate and efficient estimation of canopy fuel characteristics over large areas of forests (Andersen et al., 2005). LIDAR sensors are high resolution, active remote sensing tools that use lasers to measure the distance between the sensor and the object sensed (Wagner et al., 2004). This technology is useful for obtaining accurate, high resolution measurements of surface elevations (Bufton et al., 1991). In addition, airborne LIDAR data can provide new information about the canopy surface and vegetation parameters such as height, stem density, crown dimensions, volume and biomass (Naesset and Okland, 2002; Popescu and Wynne, 2003; Nelson et al., 2003; Popescu et al., 2004). Operationally, LIDAR ranging data are commonly used for precise terrain elevation characterization.

Important assessments include the potential size, rate, and intensity of a wildland fire, which can assist in short and long-term wildland fire planning and resource

distribution (Keane et al., 2000). Recent advances in computer software technology have allowed development of several spatially explicit fire behavior simulation models, which predict the spread and intensity of fire (Andrews and Queen, 1999). Some of this software can be used to predict future fire growth and compute possible parameters of wildland fires for real-time simulations (Campbell et al., 1995, Richards, 1990). An example of such software is FARSITE (Fire Area Simulator), a spatially explicit fire growth model developed by Finney (1994). FARSITE is a two-dimensional deterministic model for simulating the spatial and temporal spread and behavior of fires under conditions of heterogeneous terrain, fuels, and weather (Finney, 1998). This software incorporates models for surface fire (Rothermel, 1972), crown fire (Wagner, 1993), spotting (Albini 1979), fire acceleration, and fuel moisture. FARSITE produces maps of fire growth and behavior in vector and raster format (Stratton, 2004). The software's simulator is the useful tool to evaluate fuel treatments. In addition, to calculate surface fire spread, FARSITE implements the Rothermel (1972) equations (Miller and Yool, 2002). Many wildland fire managers use this software to simulate characteristics of prescribed wildfires (Finney 1998, Grupe 1998).

This study demonstrates the importance of using accurate maps of fuel models derived using new LIDAR remote sensing techniques.

Objectives

This study has two main objectives.

(1) The first objective is to develop a methodology to use LIDAR and multispectral remote sensing to accurately and effectively assess fuel models in East Texas. The specific objectives:

- develop LIDAR-derived products and the methodology to use them for assessing fuel models;
- investigate the use of several techniques for data fusion of LIDAR and multispectral imagery for assessing fuel models;
- investigate the accuracy of fuel maps generated using LIDAR as opposed to the generation of fuel maps from satellite imagery alone; and
- produce spatially explicit digital fuel maps.

(2) The second objective is to model fire behavior using FARSITE and investigate differences in modeling outputs using fuel model maps, which differ in accuracy, in east Texas.

Thesis Organization

The thesis consists of five chapters. An introduction to the thesis is presented here. Chapter II contains a literature review about fuel models and FARSITE studies. Chapter III contains an introduction, a discussion on methodology for mapping surface fuel models using LIDAR and multispectral data and it includes findings of the study. In Chapter IV, FARSITE simulation software was run with two different datasets. This

chapter also includes introduction, methodology and results sections. Conclusions of the study are presented in Chapter V.

CHAPTER II

LITERATURE REVIEW

There is a limited number of studies in the literature that used airborne scanning laser (LIDAR) systems to estimate forest fuels parameters. Most studies map vegetation, then assign fuel models to the vegetation classification. De Vasconcelos and others (1998) mapped the Anderson (1982) fuel models in north-central Portugal using neural network pattern searching on elevation, land use, and satellite imagery layers. They found this method strongly differentiated between grassland and shrubland fuel models with accuracies between 33 to 75 percent depending on land cover type. Their study emphasized the importance of ground data to train, test, and validate the neural networks. Riano's (2003) study has demonstrated a semi-automated technique can be used to extract forest fuel distribution from LIDAR data in forests dominated by conifer and deciduous tree species. The results demonstrated that LIDAR can provide detailed spatial information on forest attributes relevant to fire behavior that may also be used for direct input into spatial fire behavior models. Baath et al. (2002) developed an approach to obtain practical information about recent and future forest fuel potentials. Morsdorf et al. (2004) used a k-means clustering algorithm to measure individual tree crown dimensions for forest fire risk assessment in Switzerland. Roberts et al. (1998) used AVIRIS (Airborne Visible Infra-Red Imaging Spectrometer) airborne sensor imagery and spectral mixture analysis to classify vegetation fraction, cover, and water content which were then related to fuel loadings directly sampled on the ground. In Andersen et al. (2005) study, regression analysis was used to develop predictive models relating a

variety of LIDAR-based metrics to the canopy fuel parameters estimated from inventory data collected at plots established within stands of varying condition within Capitol State Forest, in western Washington State. Mark et al. (1995) assigned Anderson (1982) fuel models to combinations of timber size class, stocking level, crown density, crown texture, and vegetation type that were sampled or extrapolated attributes of photo-interpreted polygons in their timber stand atlases.

Recently, FARSITE has been used by many fire managers all over the world (Finney 1998, Keane et al., 1998). Falkowski et al.(2005) evaluated the accuracy and utility of imagery from the Advanced Spaceborne Thermal Emission and Reflection radiometer (ASTER) satellite sensor, and gradient modeling, for mapping fuel layers for fire behavior modeling with FARSITE and FLAMMAP. They mapped the surface fuel models (National Forest Fire Laboratory (NFFL) 1–13) using a classification tree based upon three gradient layers; potential vegetation type, cover type, and structural stage. The final surface fuel model layer had an overall accuracy of 0.632. Stephens (1997) used FARSITE to spatially simulate fire growth and behavior in mixed-conifer forest and to investigate how silvicultural and fuels treatments affect potential fire behavior in the North Crane Creek watershed of Yosemite National Park. Keane et al. (2000) used FARSITE to spatially model fire behavior on the Gila National Forest, New Mexico. They used sampled field data to guide the classification criteria for each category and to assess the value of each category to the overall classification and mapping effort in a spatial context. They coded all vegetation classifications into Paradox database queries that use plant species and canopy cover information along with other relevant site

descriptions. The coded plots were then used to assign the FARSITE fuel and crown characteristics parameters to each layer to finally create the FARSITE input layers. Basically, they developed all the spatial data layers required by FARSITE. Stratton (2004) used FireFamily Plus to evaluate historical weather and calculate seasonal severity and percentile reports. Then they used this information in FARSITE and FlamMap to model pre-treatment and post-treatment effects on fire growth, spotting, fireline intensity, surface flame length, and the occurrence of crown fire. Miller and Yool (2002) evaluated the sensitivity of FARSITE to the level of detail in the fuels data, both spatially and quantitatively, which provided land managers knowledge about the effectiveness of detailed fuels mapping in modeling fire spread.

The current study builds on and extends the research efforts described above by integrating LIDAR and multispectral data to develop fuel models. We employ a unique approach to classify fuel models based on LIDAR height bins and optical imagery, and we use the various LIDAR-based and scanner-based data layers to set initial conditions for fire simulations using FARSITE. We developed all the spatial data layers, fuel model map, canopy cover, DEM, slope and aspect, required by FARSITE using LIDAR remote sensing techniques and multispectral data. In addition, we are looking into more fuel models in a large area, covering 4,741.83 ha. Different image processing approaches were used to improve the overall accuracy of image classification and our accuracy assessment results are higher than results of the other studies.

CHAPTER III

MAPPING SURFACE FUEL MODELS USING LIDAR AND MULTISPECTRAL DATA FUSION

Introduction

Surface fuels are greatest concern because they are primary contributors to the intensity and spread of fires. According to Anderson (1982), surface fuels have been classified into four groups: grasses, brush, timber, and slash. Fire behavior can differ if there is a direct relationship between the fuel load and its distribution among the fuel particle size classes (Anderson, 1982). A fuel model is a simulated fuel complex for which all the fuel loadings, common sizes, and arrangements have been specified for solution of a mathematical fire spread model (Reeves, 1988). A total of thirteen surface fuel models are identified for the United States, each varying in amount, size, and arrangement of the fuel model (Anderson, 1982). A total of seven fuel models are available in our study area: grass fuel models 1 and 2, brush fuel model 4, 5, and 7, and timber litter fuel model 8 and 9. Fig. 1(a), (b), and (c) represents the types of fuel models which are available in the study area. Fuel models are one of the inputs into fire simulation software, which help the user reasonably estimate fire behavior (Reeves, 1988).

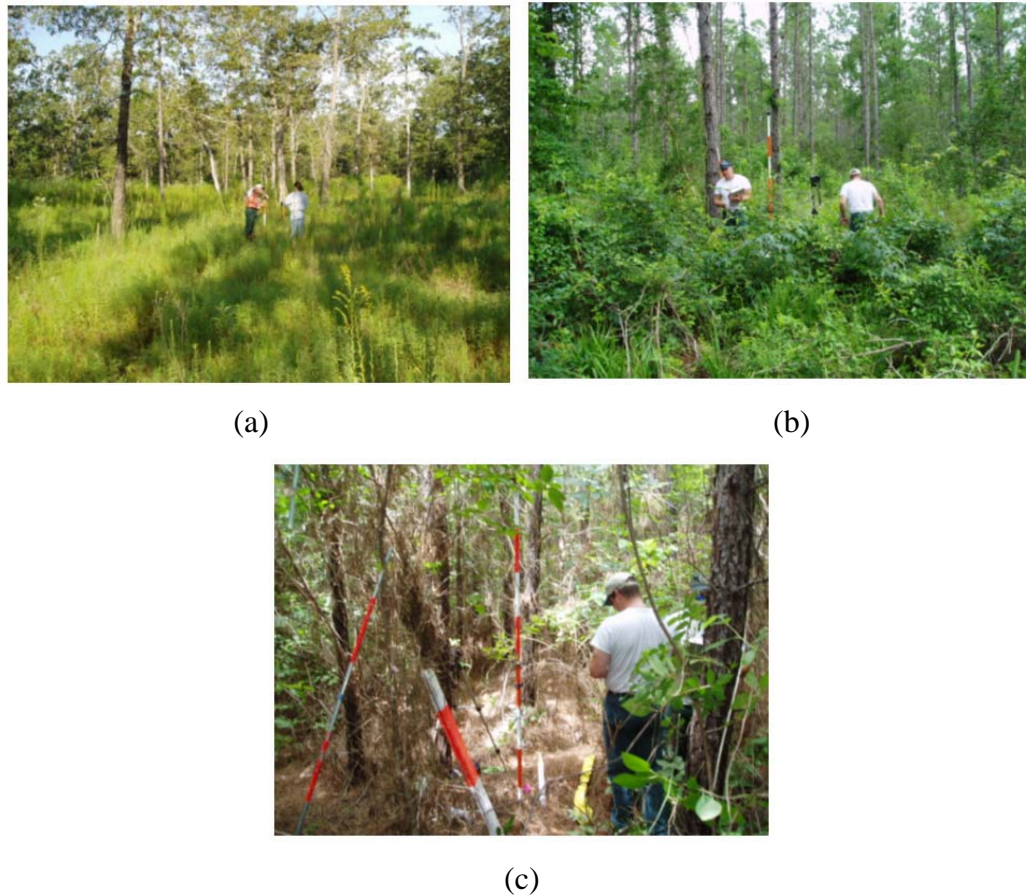


Fig. 3. 1. Example of (a) grass fuel model, (b) brush fuel model, and (c) timber fuel model on the study area.

Multispectral image classification is an important technique of remote sensing and image analysis. There are different ways to perform classification such as supervised or unsupervised, parametric or nonparametric, and contextual or noncontextual (Keuchel et al., 2003). Maximum Likelihood and Mahalanobis Distance that are decision rules methods of supervised image classification were used to determine which classifier is more efficient and useful for this study. In a supervised image classification, some of the land-cover types such as forest, urban, water, and

agriculture are known (Hodgson et al., 2003). To classify remotely sensed data successfully, supervised classification training sites must be carefully assigned to land-use and land-cover information (Lunetta et al., 1991; Congalton and Green, 1999). In this chapter, two different fuel model maps, one from LIDAR-derived data and the other one from multispectral imagery, were obtained and comparisons of results were presented.

The overall aim of this chapter is to develop the use of Light Detection and Ranging (LIDAR) remote sensing to accurately and effectively assess fuel models in East Texas. More specific objectives include: (1) developing LIDAR derived products and the methodology to use them for assessing fuel models; (2) investigating the use of several techniques for data fusion of LIDAR and multispectral imagery for assessing fuel models; (3) investigating the gain in fuels mapping accuracy when using LIDAR as opposed to QuickBird imagery alone; and (4) producing spatially explicit digital fuel maps.

Materials and Methods

Study Area

The study area is centered within the rectangle defined by 95° 24' 57" W- 30° 39' 36" N and 95° 21' 33" W- 30° 44' 12" N, covering 4,741.83 ha, in east Texas near Huntsville. Forest stands are in various stages of development which include pine, pine-hardwood mixed stands, and hardwood stands in the study area. The study area also includes open ground with fuels consisting of grasses and brushes. Fig. 3.2 represents the QuickBird image, a high-resolution satellite owned and operated by DigitalGlobe

with 2.5x2.5m resolution. Yellow marks on the image represent the field plot locations over the study area.

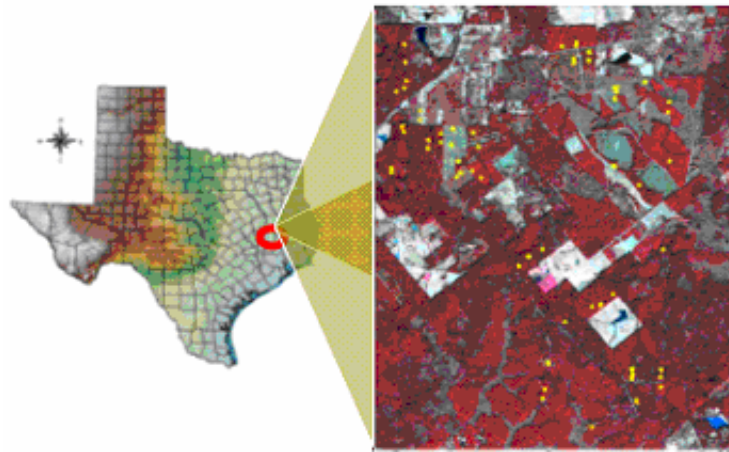


Fig. 3. 2. Map of Texas indicating the location of our study area and false color composite of a QuickBird image, with field plot locations.

Data

Three types of data were used in this project: LIDAR data, in-situ data, and multispectral QuickBird data.

LIDAR Data

LIDAR scanning data was provided by M7 Visual Intelligence Inc. in LAS format. The LAS file format is a binary file format that maintains information specific to the LIDAR nature of the data while not being overly complex. LIDAR data were acquired over an area of 6,474.9 hectare (25 square miles) in leaf off condition during March 2004. M7 Visual Intelligence Inc. uses semi-automated process for processing

GPS and LIDAR data that includes built-in measures for quality control and assurance throughout each step of the process. A total of 47 flight lines were collected over the study area, with 28 flight lines obtained from East to West and 19 flight lines obtained from North to South. An average of 2.58 points/m² and a maximum of 39.84 points/m² were found. Fig. 3.3 shows the flight lines over the study area. This flight line arrangement with complete LIDAR coverage from two different directions was designed to allow a good penetration of laser shots to the ground for characterizing surface fuels and to reduce effects of row direction on pine plantations.

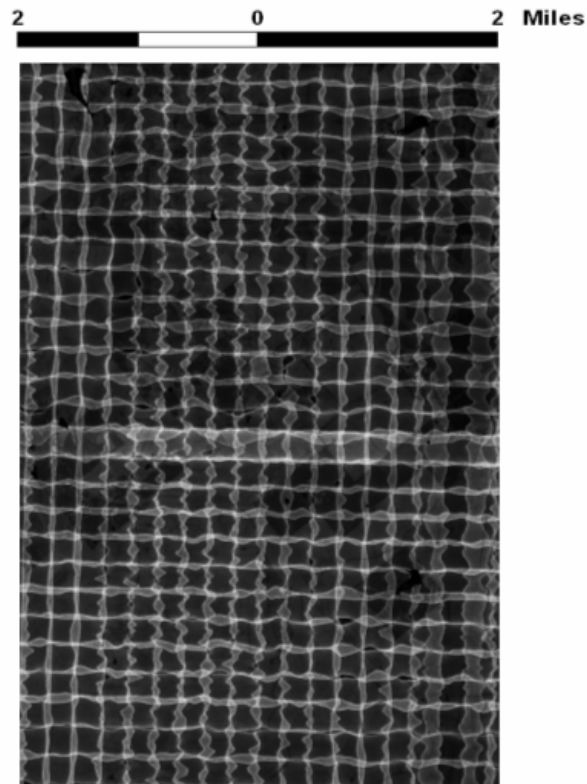


Fig. 3.3. Flight lines over the Huntsville area.

Ground Inventory Data

In order to assess fuel models and forest inventory parameters and determine the accuracy of airborne LIDAR estimates, in-situ data were gathered for this study from May 2004 to July 2004. A total of 62 plots including a total of 1005 trees were measured in the study area. Potential plot locations were initially identified using ground reconnaissance to ensure adequate sampling of the common fuel types in east Texas. This strategy was used due to the difficulty of identifying fuels based solely on Quickbird satellite imagery. After several potential sites were located on the ground, random plot locations within these stands were generated in the office.

A 404.6 m² (1/10th acre) circular plot with a radius of 11.35 m (37.24ft) was established for all forested and non-forested plots, except for the ones located in unthinned pine plantations. Because of the uniformity of trees in unthinned plantations, a smaller plot size of 40.468 m² (1/100-acre) with a radius of 3.59 m (11.78ft) was used.

Plots were located in the field by obtaining a distance and direction from an identifiable feature on the Quickbird imagery and using a compass to chain in. This method was preferred over GPS navigation because of poor GPS satellite reception underneath the forest canopy (necessary precautions were taken to prevent plot location bias). Once the plot center was established, the coordinates were recorded with a GeoExplorerXT. A minimum of 30 positions were collected for each plot and saved to the GeoXT so they could be differentially corrected later using Trimble's Pathfinder software. A 3.66 m (12 ft) to 4.88 m (16 ft) antenna had to be used on most forested plots in order to receive an adequate GPS signal.

All trees were measured and species were identified within the plot boundaries. Each tree location was mapped using distance and azimuth from plot center. Tree distance was measured to the nearest 3 cm (0.1 ft) using a Hagl f Vertex III Hypsometer and azimuth was measured to the nearest degree.

Fuel models can be quickly estimated by taking a photo series including detailed data for each fuel complex shown (Reeves, 1988). Six digital photographs were taken from each plot center, with two photos taken from a general view and four photos taken facing north, south, east, and west directions. Fig. 3.4 (a) represents the location of Plot #8 in the study area and fig. 3.4 (b) represents the digital photos that are taken from the plot center facing north, south, east, and west. These photos were then evaluated to assess fuel models (Reeves, 1988, and Anderson, 1982).

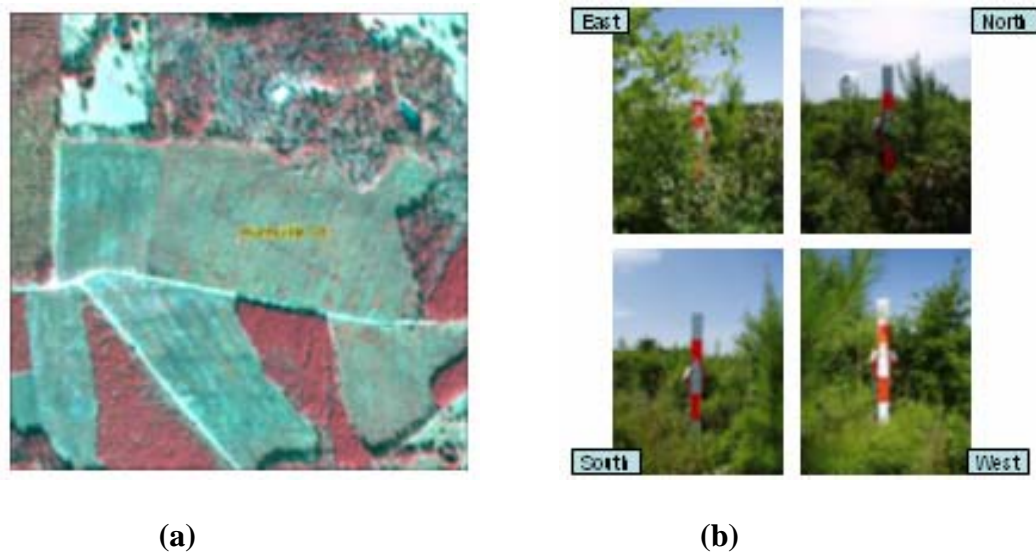


Fig. 3.4. (a) Location of Plot #8 in the study area shown on the QuickBird image, (b) digital photos of Plot #8.

Each plot's fuel model type was determined by specialists from Texas Forest Service personnel involved with fire behavior and mitigation efforts. Each of the four photographs available for each plot as well as field inventory data were analyzed to determine fuel models. A total of seven fuel models are available in our study area: Fuel model 1, Fuel model 2, Fuel model 4, Fuel model 5, Fuel model 7, Fuel model 8, and Fuel model 9. Table 3.1 represents the description of each fuel model type.

Table 3.1
Description of fuel models.

Fuel Model	Typical Fuel Complex
Grass and grass-dominated	
1	Short grass (foot)
2	Timber (grass-understory)
Chapparral and shrub fields	
4	Chapparral (6 feet)
5	Brush (2 feet)
7	Southern rough
Timber litter	
8	Closed timber litter
9	Hardwood litter

Processing Approach

The overall study steps to derive fuel maps are illustrated in Fig. 3.5.

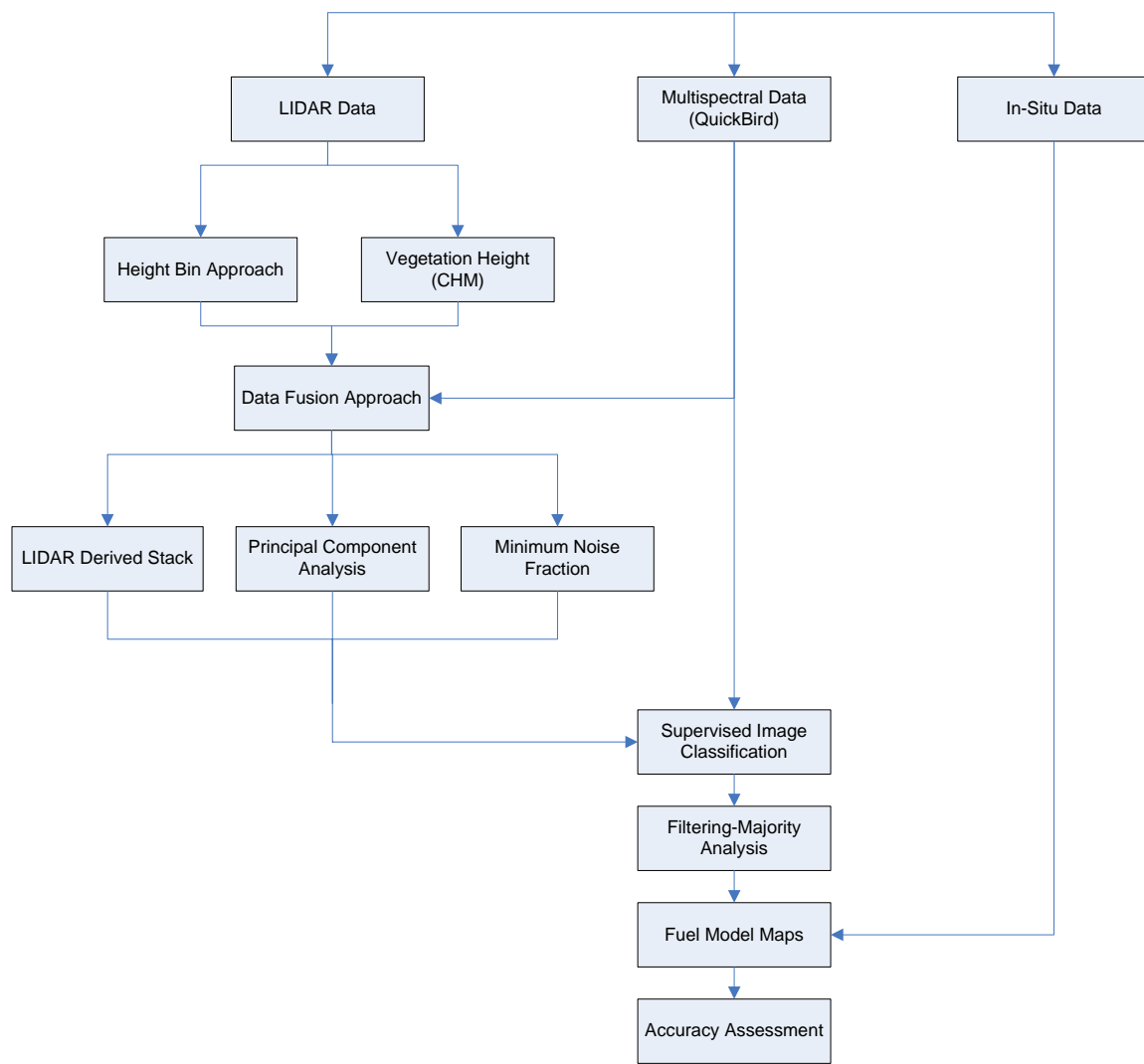


Fig. 3.5. The flowchart of processing approach.

Height Bins Approach

The height bin approach was used to generate LIDAR multiband data from scanning data. The height bins approach makes use of the entire LIDAR point cloud. LIDAR bins were created by counting the occurrence number of LIDAR points within

each volume unit and normalizing by the total number of points. The percentage of LIDAR hits can be obtained for any height interval. Fig. 3.6(a) represents 3D distribution of laser hits of Plot 9, Fig. 3.6(b) shows the zoom in view of Plot 9, and Fig. 3.6(c) represents the digital photograph that was taken from the area.

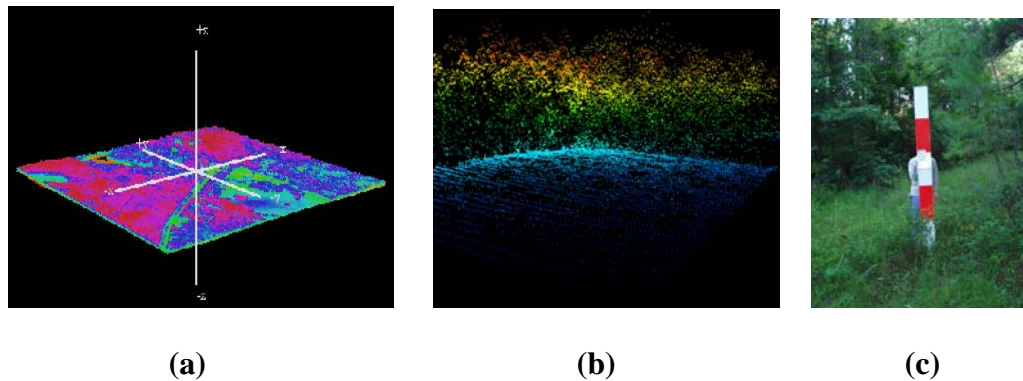


Fig. 3.6. (a) The 3D of laser hits of Plot 9, (b) zoom in view of Plot 9, and (c) the digital photograph from the area.

A total of eleven LIDAR height bins were obtained and Fig. 3.7 illustrates the output of this process. The first five height bins are generated for 0.5 m height intervals to afford a better characterization of vegetation that defines surface fuels. The upper bins are spaced at 3 m and 5 m, band 6 to 10. The last bin is generated from laser hits above 30 m.

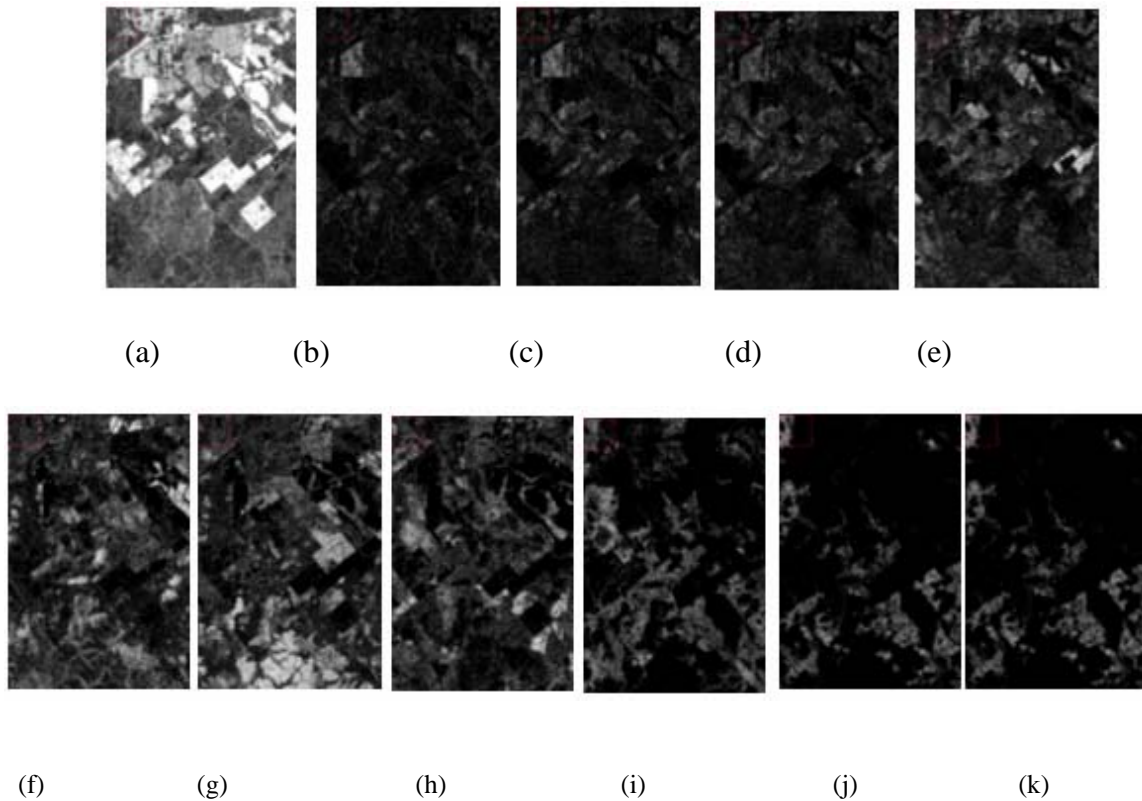


Fig. 3.7. Overall view of the eleven Height Bins. (a) Bin 1: 0-0.5 m, (b) Bin 2: 0.5-1.0 m, (c) Bin 3: 1.0-1.5 m, (d) Bin 4: 1.5-2.0 m, (e) Bin 5: 2.0-2.5 m, (f) Bin 6: 2.5-5.0 m, (g) Bin 7: 5.0-10.0 m, (h) Bin 8: 10.0-15.0 m, (i) Bin 9: 15.0-20.0 m, (j) Bin 10: 20.0-25.0 m, (k) Bin 11: >30.0 m.

Data Fusion Approach

Data fusion deals with association, correlation, and combination of information and data from one or many sources (Llinas, 2002). In this study, three different data fusion approaches were used: LIDAR-multispectral stack, principal component analysis, and minimum noise fraction (MNF). A new image, LIDAR-QuickBird stack image of ten bands, was created by stacking the four bands of the QuickBird image with four

LIDAR height bins, one band from the canopy cover model, and one band from the canopy cover variance and the resolution of our data is 2.5 m x 2.5 m. Principal Component Analysis (PCA) is a helpful statistical technique that is used to produce uncorrelated output bands, to segregate noise components, and to reduce the dimensionality of data sets (Jensen, 2005). The MNF transform is used to determine the inherent dimensionality of image data, to segregate noise in the data, and to reduce the computational requirements for subsequent processing (Boardman and Kruse, 1994). The MNF method is similar to PCA that has been used for a long time in multispectral image processing. We investigated both principal components and minimum noise fraction to create new fused images. We then applied supervised image classification on the new images, examined its effect for improving overall classification accuracy, and finally compared results. The reason we used MNF and PCA methods is to reduce the noise, produce uncorrelated output bands, and to reduce the dimensionality of the dataset.

LIDAR-derived Stack

By using ENVI 4.2 (Research Systems, Inc.) we built a new multiband image. This image includes a total of 10 bands and will be subsequently referred to as the LIDAR-QuickBird Stack. As is shown in Fig. 3.8, the first four bands are taken from the Quickbird image, the fifth band is LIDAR derived canopy cover, sixth, seventh, eighth, and ninth bands are obtained from the first four LIDAR Height Bins (0-0.5, 0.5-1.0, 1.0-1.5, 1.5-2.0 meters), and the last band is obtained from canopy height model variance. We used only the first four LIDAR bins by assuming they characterize best

the vertical structure of surface fuels within a 2m vertical canopy space adjacent to the ground.

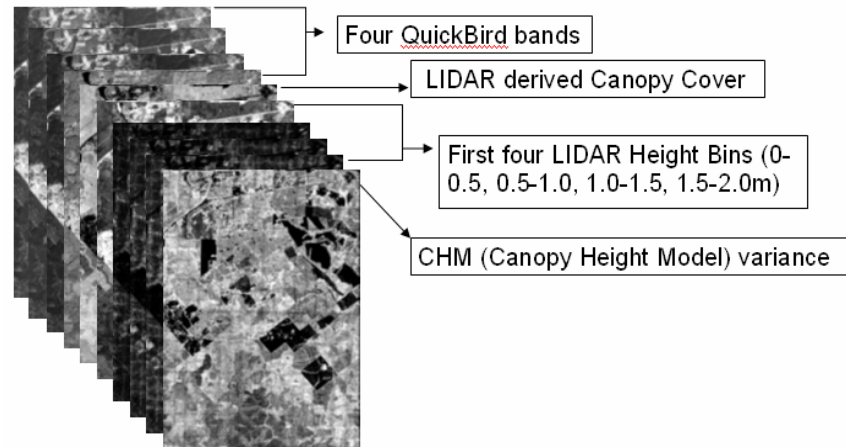


Fig. 3.8. The LIDAR-QuickBird stack image

Principal Component Analysis (PCA)

PCA was applied to the LIDAR-QuickBird stack image, which has ten bands. We used the first five of the ten PCs for our subsequent image classification. Fig. 3.9 illustrates the first five PCs. The PCA transformation is based on the variance and covariance of the data set.

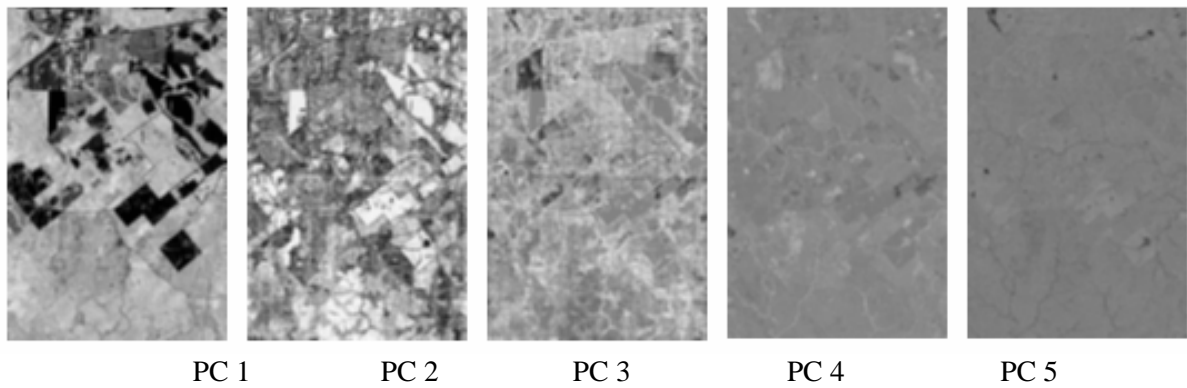


Fig. 3.9. First five PC images.

The variance is a measure of the scatter or spread within one variable of the data set, and the covariance is a measure of the scatter between two variables of a data set (Smith, 2002). Eigenvalues, variance, and eigenvector were extracted for each PC. Table 3.2 represents the percentage of total variance, eigenvalues, and cumulative variance explained by each principal component. The first principal component accounts for 88.97% of variance in the entire LIDAR and multispectral dataset. In addition, the first five components that we used for image classification account for approximately 99 percent of the total variance. It can be concluded that the first five principal components can replace the original ten bands of the LIDAR-QuickBird stack image, while reducing the size of the data set, redundancy, and noise.

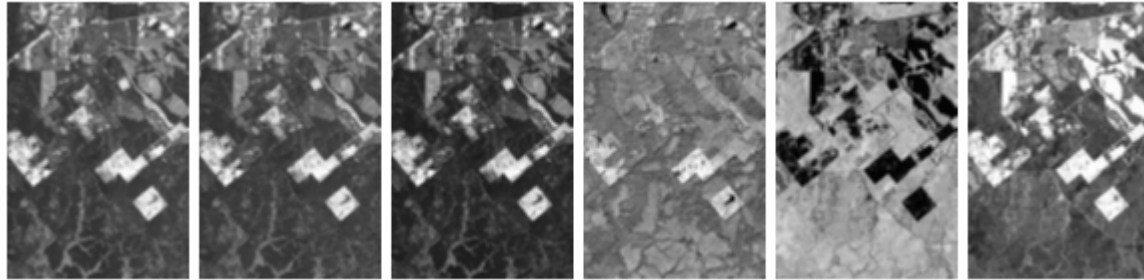
Table 3.2
Calculations of Eigenvalues, percentage of total variance and cumulative variance for each PC.

PCs	Eigenvalue	% of total Variance	Cumulative
PC1	873676.7	88.97	88.97
PC2	53848.92	5.48	94.46
PC3	31214.62	3.17	97.63
PC4	7711.736	0.78	98.42
PC5	6495.253	0.66	99.08

Minimum Noise Fraction (MNF)

MNF was applied to the LIDAR-QuickBird stack image that has ten bands. MNF determines the dimensionality of image data, separates noise in the data, and reduces the computational requirements for processing (Boardman and Kruse, 1994). The MNF transform has two Principal components transformations (Green et al. 1988). The first transformation is based on an estimated noise covariance matrix. This transformation rescales and decorrelates any noise in the data. Results obtained from this step in transformed data in which the noise has unit variance and no band-to-band correlations. Principal components transformation is the second step that creates new bands containing the majority of the information. By examination of the eigenvalues, the inherent dimensionality of an image can be determined (ENVI, 2003). Since PCA transformation maximizes the variance, we applied MNF to our data. Instead of maximizing the variance, we can use MNF to maximize the signal to noise ratio (SNR)

(Canty, M.J,70-71, 2006). Six of the ten MNF bands were stacked, and each band is shown in Fig. 3.10.



MNF 1 MNF 2 MNF 3 MNF 4 MNF 5 MNF 6

Fig. 3.10. MNF images.

Eigenvalues, percentage of variance, and cumulative variance were calculated for each MNF band as is shown in Table 3.3. The table shows that the first six MNF bands account for approximately 97 percent of the total variance. As such, we decided to use the first six components of the MNF band transformed image for our subsequent processing.

Table 3.3
Calculations of Eigenvalues, percentage of total variance and cumulative variance for each MNF.

MNF	Eigenvalue	% of total VAR	Cumulative
MNF1	183.95	83.33	83.33
MNF2	17.14	7.76	91.1
MNF3	5.33	2.41	93.52
MNF4	4.01	1.81	95.34
MNF5	3.02	1.36	96.71
MNF6	2.01	0.91	97.62

Image Processing

The first step in undertaking a supervised classification is to define the areas that will be used as training sites for each fuel model class. Seven initial classes were considered and classification accuracy was evaluated using confusion matrix and K-hat statistics. The Region of interest (ROI) actually corresponds to our field plots. A plot of 11-m radius covers approximately 80 pixels, given a 2.5 m spatial resolution for our data. Thus, the 80 pixel-size resulted from collecting a circular shaped ROI over the field plot. A total of twenty-three polygons were selected which results in a total of 1840 pixels for each of the QuickBird image, LIDAR-QuickBird stack image, principal component image, and minimum noise fraction image. Then, ROI separability reports, which calculate the spectral separability between chosen ROI pairs for a given input file (Jensen, 2005), have been computed for each data set. The same ROIs chosen over the LIDAR-QuickBird stack image were used on the stack of first five PCs and stack of first six MNF component images.

Supervised image classification was performed using parametric decision rules, such as the Maximum Likelihood and the Mahalanobis Distance decision rules with the multispectral QuickBird image, the LIDAR-QuickBird stack image, the principal

component image, and the minimum noise fraction image. Image classification results in a per pixel characterization of fuels. Since we evaluated fuel models on a per plot basis, we applied a majority filter to the classified image using a 7x7 window size. We assessed the accuracy of this final map of fuel models for each data set. The Kappa statistic (Khat) derived for each classification verifies if classification results are precise (Lillesand and Kiefer, 1994, Jensen, 1996, and Congalton and Green, 1999).

Results and Discussion

The results of four classification methods and classification accuracies were assessed. Among all the supervised image classifications that we applied to our images, Maximum Likelihood yielded the best results for the multispectral QuickBird image with 76.52% overall accuracy and 0.68 kappa coefficient. Mahalanobis Distance yielded the best results for the LIDAR-QuickBird stack image with 87.17% overall accuracy and 0.83 Kappa Coefficient. Fig. 3.11(a) represents the result of multispectral QuickBird image classification; Fig. 3.11(b) illustrates the result of the LIDAR-QuickBird stack image.

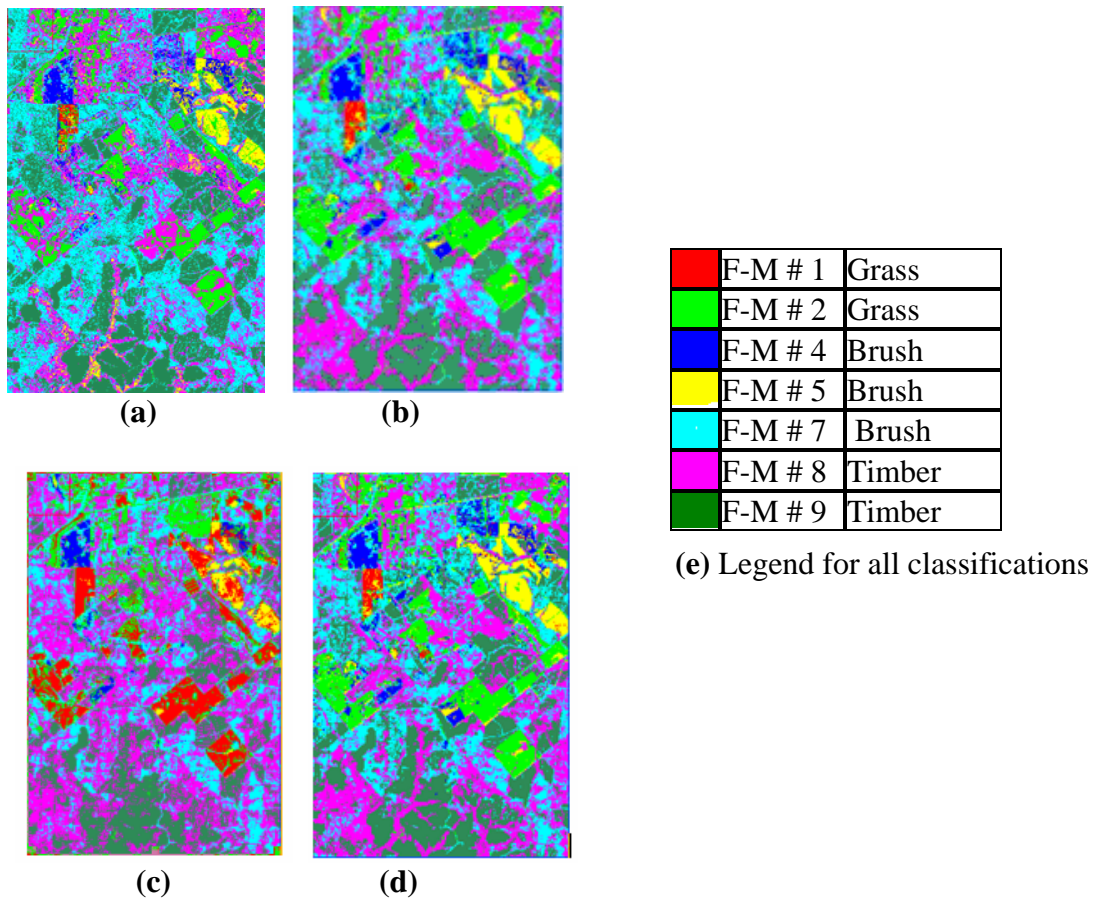


Fig. 3.11. (a) The classification result of multispectral QuickBird image, (b) the classification result of data fusion stack of LIDAR and multispectral imagery, (c) the classification result of PC stack image, (d) the classification result of MNF-fused stack image, and (e) legend for all classifications.

With the PC image, the Mahalanobis Distance classifier provided the best results. The accuracy assessment was 62.44% and the Kappa Coefficient was 0.53. Compared to the accuracy of the multispectral QuickBird and LIDAR-QuickBird stack images, the

PC stack image was less accurate. Fig. 3.11(c) represents the output of the PC stack image.

As for the MNF image, the Mahalanobis Distance decision rules classification yielded the best results of all the supervised image classification decision rules with an accuracy assessment of 90.10% and with a Kappa Coefficient of 0.86 for a new MNF-fused stack image. Fig. 3.11(d) illustrates the output of this classification process and Table 3.4 shows a comparison of results for all supervised image classifications. Compared to the multispectral QuickBird image, LIDAR-QuickBird stack, and PC stack images accuracy, MNF provided the best result by having the highest accuracy.

Table 3.4
Comparison of results for all supervised image classifications.

	Overall Accuracy	Kappa Coefficient
Multispectral QuickBird Image	76.52 %	0.68
LIDAR-QuickBird Stack Image	87.17 %	0.83
PC stack image	62.44 %	0.53
MNF stack image	90.10 %	0.86

Conclusions are given in Chapter V.

CHAPTER IV

USING LIDAR-DERIVED FUEL MAPS WITH FARSITE FOR FIRE BEHAVIOR MODELING

Introduction

FARSITE is based on spatial data, and thus it is a powerful tool for the fire manager. It also has the ability to simulate spatial and temporal changes into the fire model. FARSITE is specially designed for forest fire modeling. It allows a user to interactively specify the time, duration, and locations of a multiple ignition fire simulation (Finney, 1995).

Fuel model maps, obtained from the previous chapter, were used as inputs for FARSITE simulation software in this chapter. We applied supervised image classification to determine which classifier is more efficient and useful for two different fuel model maps. These fuel model maps include a total of seven fuel models. The first fuel model map was obtained by classifying only a high-resolution QuickBird satellite image and the second one was obtained by classifying a LIDAR and QuickBird fused data set. The results from Chapter III show that LIDAR improves the accuracy of fuel mapping by at least 13.5%.

In order to run FARSITE, spatial data derived from GIS (Geographic Information Systems) and/or remote sensing are required and should be imported into the program. Airborne LIDAR systems can assist in providing data for the FARSITE software (Chuvieco, 1997). These data layers must be reliable for all lands and

ecosystems (Keane et al., 2000). The consistency and accuracy of the input data layers are very important for realistic predictions of fire growth (Keane et al., 1998, Finney 1998). The fuel model map is the key input for the simulation model. Many fire managers do not have the fuel maps needed to run the FARSITE model for their area. Vegetation layers and databases should quantify fuel information at a high level of detail or resolution for FARSITE to work well, but this is not the case for most existing vegetation layers and databases (Keane, 2000).

The main objective of this chapter is to model fire behavior using FARSITE and investigate differences in modeling outputs using fuel model maps, which differ in accuracy, in east Texas.

Materials and Methods

Two different fuel model maps obtained from Chapter III were used to see the differences in fire growth with fuel model maps of different accuracies (see Fig. 4.1(a) and (b)).

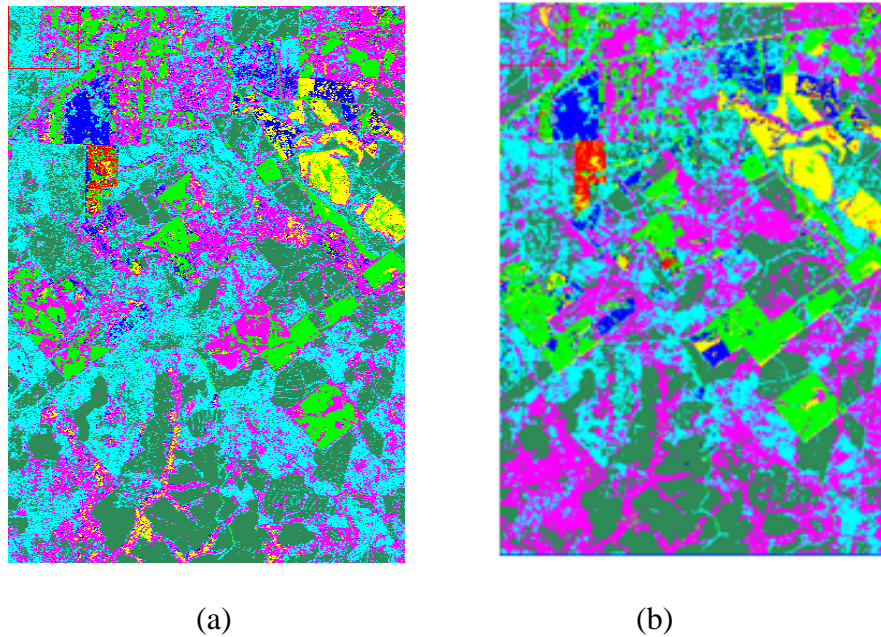


Fig. 4.1. (a) The fuel map obtained by classifying a LIDAR and QuickBird fused data set, (b) the fuel model map obtained by classifying a QuickBird image.

Data

FARSITE version 4.1 was used in this study. This software requires eight data layers including Digital Elevation Model (DEM), slope, aspect, canopy cover, fuel models map, weather, wind, and fuel moisture for surface fire simulations (Finney, 1995). Two different input data sets were used in this study to generate real-time fire simulation outputs.

Dataset with LIDAR-derived Fuel Map

We developed all the spatial data layers, which are required by FARSITE. The first fuel model map at 2.5 m resolution was derived from LIDAR and is shown in Fig.

4.1(a). Based on Chapter III's results, a LIDAR-QuickBird stack image of ten bands was created by stacking the four bands of the QuickBird image with four LIDAR height bins, one band from the canopy cover model, and one band from the canopy cover variance (see fig. 3.8.). In addition, the height bin approach was used to generate LIDAR multiband data from scanning data (Popescu and Zhao, in review). LIDAR bins were created by counting the occurrence of LIDAR points within each volume unit and normalizing by the total number of points (Popescu and Zhao, in review). A Mahalanobis distance algorithm in ENVI (ITT Visual Systems, Inc.), image processing software, was used to classify the imagery. A total of seven fuel models are available in our study area: grass fuel models 1 and 2, brush fuel model 4, 5, and 7, and timber litter fuel model 8 and 9.

Canopy cover, the horizontal percentage of area covered by tree crowns at the stand level, was found using methods developed by Griffin et al. (in review). Their study developed the use of airborne laser methods to evaluate various canopy parameters such as canopy cover and Leaf Area Index (LAI). To summarize, canopy cover is estimated by using LIDAR-derived height bins and calculating the percentage of laser canopy hits 2m above ground.

DEM was also obtained from LIDAR. By using ENVI software, slope and aspect were derived from the DEM. Weather and wind data were downloaded from the National Fire and Aviation Management Web Applications (http://www.fs.fed.us/fire/planning/nist/wims_web_userguide.htm).

Dataset with QuickBird-derived Fuel Map

The second map, shown in Fig. 4.1(b), was derived from QuickBird data at 2.5 m resolution. Based on the report from Chapter III, a maximum likelihood image classification was used to classify the multispectral image. This fuel model map also includes seven fuel models.

The DEM was downloaded from the National Fire and Aviation Management Web Applications (http://www.fs.fed.us/fire/planning/nist/wims_web_userguide.htm). at 30 meter resolutions, and then converted to 2.5 meter resolution. The slope and aspect data were derived from the DEM, using ENVI. Weather and wind data were also downloaded from the National Fire and Aviation Management Web Applications (http://www.fs.fed.us/fire/planning/nist/wims_web_userguide.htm). Canopy cover and fuel moisture were developed based on field data. A total of 62 plots including a total of 1005 trees were measured in the study area (see Chapter III for more detailed information).

Fire Simulation

FARSITE requires data input in ASCII file format. The reason for using ASCII text files is that these files can be viewed or created with any text editor or word processor (Finney, 1995). Since all the data were in the Band Sequential (BSQ) file format, the data were saved in ERDAS (Leica Atlanta, Georgia) image processing software image file format then converted to ARC GRID format for incorporation into the development and implementation of the fire behavior model.

A total of 62 plots were measured in the study area and plot center locations were used as ignition points with FARSITE simulations. FARSITE was run 124 times, 62 times on the dataset with the MNF-fused stack fuel model map and 62 times on the dataset with the QuickBird-derived fuel map. Fig. 4.2 shows a screenshot from the FARSITE simulation. The duration of each simulation was 72 hours beginning at 8:00 AM and ending at 8:00 AM three days later. Weather and wind data, which occurred on January 14, were used for all runs of FARSITE.

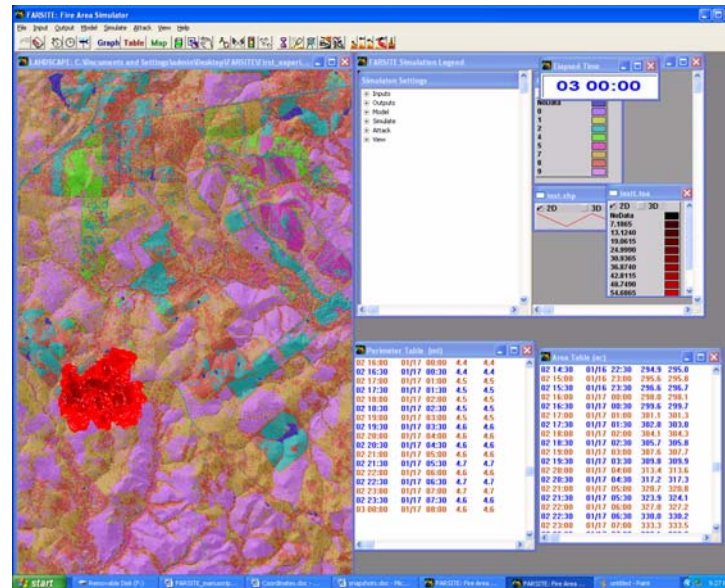


Fig. 4.2. Screenshot from the fire simulation.

Processing Approach

The overall study steps are shown in Figure 4.3.

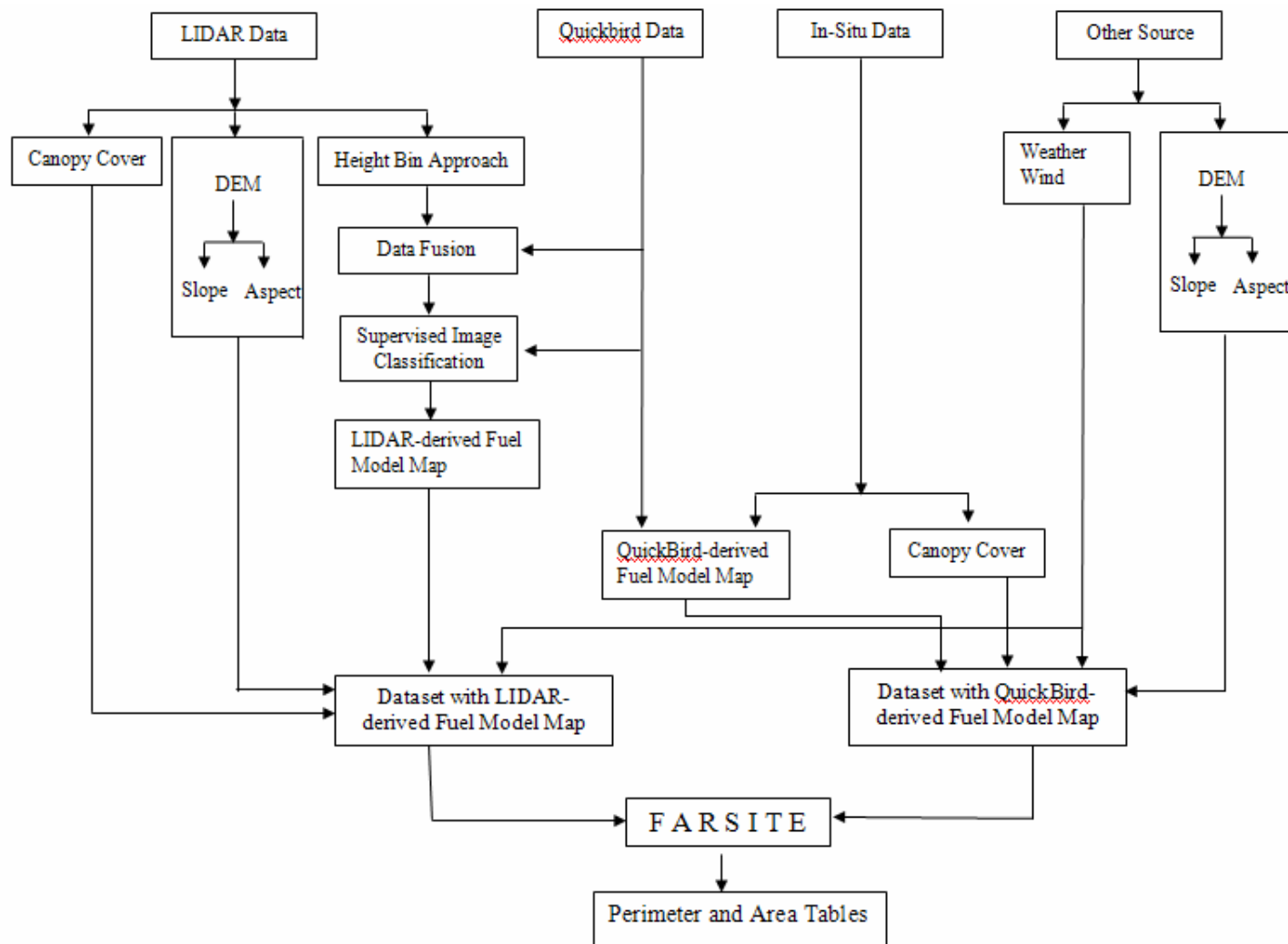


Fig. 4.3. Flow diagram illustrating the general procedure used to create the FARSITE inputs for both datasets

Results and Discussion

Different accuracy maps provided different results depending on fuel model on the study area, which were expected. However, the difference is much greater than we expected. The average burn area time for fires in Texas is between 3-5 days (Mark Stanford, personal communication, October, 2006). We have decided to run the simulation for 72 hours. The comparisons of the burned area results for 72 hours are illustrated in Fig. 4.4. Fig. 4.5 demonstrates the comparison of the fire perimeters between the two maps for 72 hours. Based upon the fire simulation results, fuel model map derived from LIDAR shows larger fire growth areas than the other fuel model map derived from QuickBird imagery.

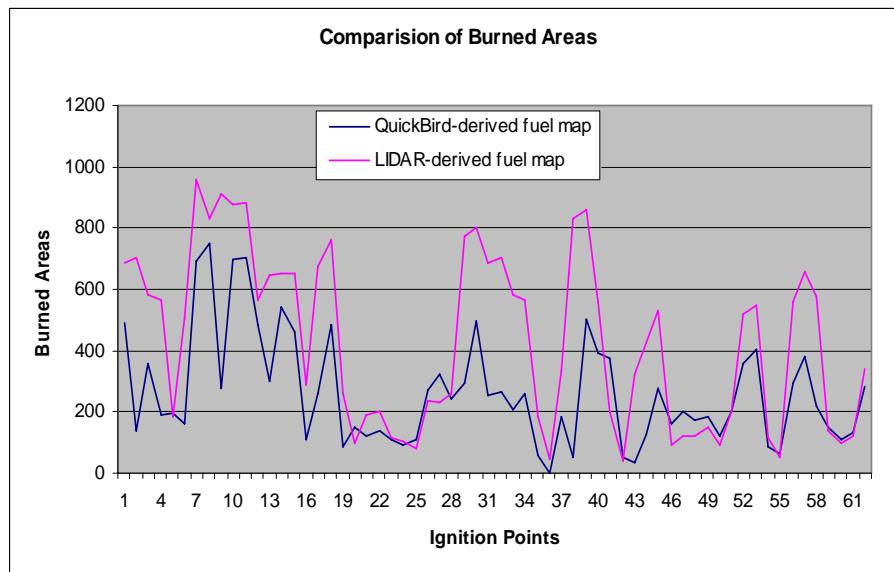


Fig. 4.4. Comparison of burned areas for both fuel model maps.

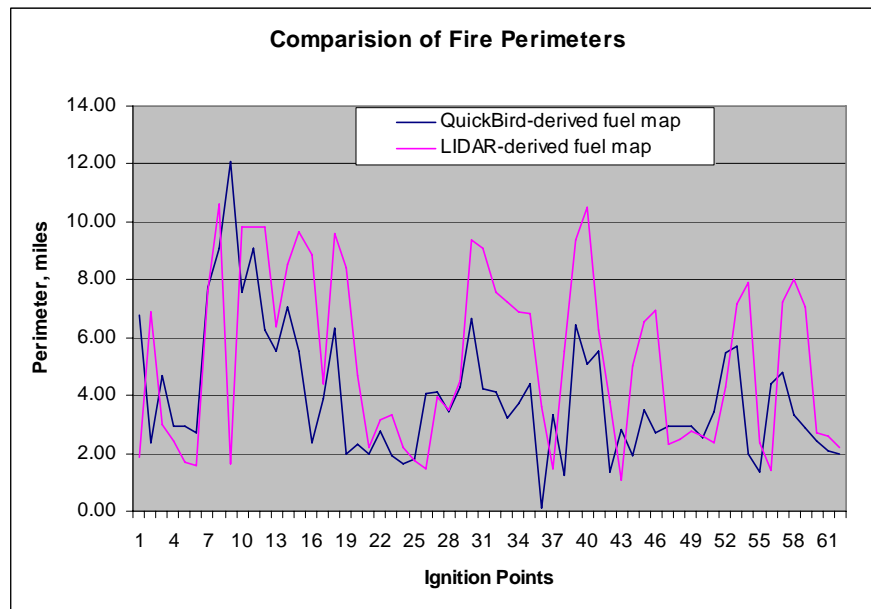


Fig. 4.5. Comparison of fire perimeter results for both fuel model maps.

The estimated average fire growth areas from LIDAR-derived fuel model map and QuickBird derived fuel model map were approximately 174.261 ha (430.593 ac) and 106.447 ha (263.026 ac), respectively. Apparently, there is a considerable difference between the two outputs. There are some extreme situations in our results. For instants, while 285.17 ha were burned on LIDAR-derived fuel model map on second run, 56.92 ha were burned on QuickBird-derived fuel model map. On the forty-third run, the burned area is 129.667 ha on the LIDAR-derived fuel model map and 13.723 ha on the QuickBird-derived fuel model map. In this case, LIDAR-derived fuel model map shows almost ten times larger burned area than the QuickBird-derived fuel model map. The reason for the difference is because maps show different fuel models on the second

ignition points, Fuel Model #2, grass group, on LIDAR-derived fuel model map and Fuel Model #8, timber litter group, on QuickBird-derived fuel model map. The same situation can be seen in Fig. 4.6 for fire perimeters for both models.

Cost of fire is one of the biggest issues. Wildfires can have significant local economic effects both long-term and short-term. Donovan and Rideout (2003) used the Cost plus Net Value Change (C+NVC) model which minimizes the cost of wildfire by minimizing the sum of presuppression (expenditures on wildfire management prior to a fire season), suppression (direct wildfire suppression expenditures during a fire season), and NVC (net wildfire damages). They assume that the cost of fire per a hectare is \$100. Resources, such as crews, dozer, engine, tractor, cost approximately \$3,800. The sum of all costs and damages is minimized. In our case, if we take a look at the results, average burned area is 174.26 ha on LIDAR-derived fuel model map. This burned area will cost around \$87,826 by summing “\$3800+\$66600+\$17426” based on Donovan and Rideout’s calculations. In this case, the NVC is \$17,426 which was calculated multiplying the total burned area with 100. Table 4.1 shows the fire fighting resources needed for a 72 hour burn time based on the LIDAR-derived fuel model map. However, the average burned area is 106.44 ha on QuickBird-derived fuel model map and the cost of fire is \$59,744. Since the average burned area on the QuickBird fuel model map is smaller than that on the LIDAR-derived fuel model map, we created another fire fighting resources table (Table 4.2) for a 72 hour burn based on the QuickBird-derived fuel model map, using fewer fire fighting resources. Apparently, there is a significant difference between these two outputs.

Table 4.1
Fire fighting resource characteristics for LIDAR-derived fuel model map.

Resource (equipment) Costs			
Resource	Pre	Cost/hr	Cost / 72 hrs
Dozer	\$300	175	\$12600
Tractor plow	\$500	150	\$10800
Type I crew	\$500	125	\$9000
Type II crew	\$600	175	\$12600
Engine#1	\$400	75	\$5400
Engine#2	\$900	100	\$7200
Engine#3	\$600	125	\$9000
TOTAL	\$3800		\$66600

Table 4.2
Fire fighting resource characteristics for QuickBird-derived fuel model map.

Resource (equipment) Costs			
Resource	Pre	Cost/hr	Cost / 72 hrs
Dozer	300	175	12600
Tractor plow	500	150	10800
Type I crew	500	125	9000
Engine#1	400	75	5400
Engine#2	600	125	9000
TOTAL	2300		46800

Conclusions are given in Chapter V.

CHAPTER V

CONCLUSIONS

Airborne LIDAR systems can be used for fire detection, location, and mapping (Justice et al., 1993), for burned area assessment, and, important to this study, for fuel mapping (Keane et al., 1998). Chapter III's results indicate that LIDAR can be used to generate accurate estimates of surface fuels parameters efficiently and accurately over extensive areas of forests. Innovative methods for fusing airborne LIDAR and satellite imagery, QuickBird, were developed, which resulted in increased accuracy for classification of surface fuels. The parametric methods Maximum Likelihood and Mahalanobis Distance supervised image classifications were effective in this study. The method that we developed by using LIDAR height bins fused with multispectral data has great potential for becoming a standard approach for mapping fuels with LIDAR and multispectral imagery. PCA did not provide improved results, with an accuracy of 62.44. Compared to the multispectral Quickbird image classification, the MNF-fused stack image, which has LIDAR-derived components, increased the overall accuracy by 13.58%. The data fusion approach, combining LIDAR and multispectral QuickBird imagery, improves the overall accuracy of image classification of fuels.

Results from the chapter IV indicate the influence of a more accurate fuel map on modeling fire behavior and assessing fire risk. According to results, LIDAR derived products were able to assess fuel models with high accuracy and it provided different information about characteristics of fire perimeters and fire growth areas. For fire mitigation purpose, we need to know both fire perimeters and fire growth areas. Fire

growth area results are helpful to determine the cost of fire. Fire perimeter results are important because they help in determining an optimal mix of fire fighting resources needed to fight fires such as dozer, tractor, crews, helicopter, engines, hourly cost of operating the resources, arrival time etc. Using two different datasets, one derived from LIDAR and the other one derived from QuickBird imagery and different data sources, provided significantly different outputs. The differences could be attributed to different fuel model map, canopy cover, DEM, slope, and aspect.

The cost of our LIDAR data were around \$32,645 and the QuickBird data were obtained for an approximate cost of \$3,890 for the whole study area, 4741.83 ha. The cost of first fuel model map which includes LIDAR and QuickBird data is \$36,535. The cost of second fuel model map which includes only QuickBird data is \$3,890. Based on this, LIDAR-derived fuel model map is more expensive than QuickBird-derived fuel models map. However, if we look at the results LIDAR data will save us thousands of dollars. The cost of LIDAR data for whole study area is a lot less than the cost of average burned areas.

Accurate estimation of fire growth area and the direction of fire growth is extremely important information for the fire management process. Knowing this essential information will avoid any health risk for local people who live in that vicinity. This information will be more useful if it is used by fire management authorities. In case of fire, if the fire managers use the QuickBird-derived fuel model map they may not be able to send enough sources to fight with the fire and this situation may cause more serious problems. Small errors in fuel model parameters may not be significant for small

study area; however for large study areas, small errors could accumulate over the duration of the fire simulation leading to large errors in predicted fire sizes. This study will assist fire managers with the mitigation of the harmful effects of wildfire. Also, it gives the power of sound, accurate, and efficient fire behavior modeling technology to forest fire fighters.

Resulting remote sensing methods and mapping products proved to have the potential for driving changes in forest resource management practices related to mitigating fire hazard that threatens the public, human lives, and environmental health in Texas and nationwide. Our results could significantly impact forest policy and forest resource management.

REFERENCES

- Albini, F.A. (1979). *Spot fire distance from burning trees: A predictive model*. USDA, Forest Service General Technical Report INT-56. Intermountain Forest and Range Experiment Station. Ogden, UT, 73 pp.
- Andersen, E.H., McGaughey, J., R., & Reutebuch, E.S. (2005). Estimating forest canopy fuel parameters using LIDAR data. *Remote sensing of Environment*, 94, 441-449.
- Anderson, H.E. (1982). *Aids to determining fuel models for estimating fire behavior*. USDA, Forest Service, General Technical Report INT-122. Intermountain Forest and Range Experiment Station, Ogden, UT, 4-16 pp.
- Andrews, P.L. & Queen, L.P. (1999). Fire modeling and information system technology. *International Journal of Wildland Fire*, 10(4), 343-352.
- Baath, H., Gallerspang, A., Hallyby, G., Lundstrom, A., Lofgren, P., Nilsson, M., & Stahl, G. (2002). Remote sensing, field survey and long-term forecasting: an efficient combination for local assessments of forest fuels. *Biomass and Bioenergy*, 22(3), 145-157.
- Boardman, J. W., & Kruse, F. A. (1994). Automated spectral analysis: a geological example using AVIRIS data, North Grapevine Mountains, Nevada. *ERIM 10th Thematic Conference on Geologic Remote Sensing, Environmental Research Institute of Michigan*, I-407- 418, Ann Arbor, MI.
- Buften, J.L., Garvin, B., Cavanaugh, J.F., Ramos-Izquierdo, L., Clem, T.D., & Karabill W.B. (1991). Airborne LIDAR for profiling of surface topography. *Optical Engineering*, 30, 72-78.
- Campbell, J., Weinstein, D. & Finney, M. (1995). *Forest fire behavior modeling integrating GIS and BEHAVE*. USDA, Forest Service Ecosystem Management Center Report. Thompson, J.E. (Compiler): Analysis in support of ecosystem management, Washington DC., 184-192 pp.
- Canty, M.J. (2006). Image analysis classification, and change detection in remote sensing: with algorithms for ENVI/IDL. *Taylor & Francis Group*. 70-71 pp.
- Chuvieco, E. & Congalton, R.G. (1989) Application of remote sensing and geographic information systems to forest fire hazard mapping. *Remote Sensing of Environment*, 29, 147-159.

- Chuvieco, E. (1997). A review of remote sensing methods for the study of large wildland fires. Megafires project ENV-CT96-0256. Spain.192.
- Congalton, R.G., & Green, K. (1999). Assessing the accuracy of remotely sensed data. *Principles and Practices*, Boca Raton, FL: Lewis Publishers, New York, 65 pp.
- De Vasconcelos, J.J.P., Paul, J.C.U., Silva, S., Pereira, J.M.C., Caetono, M.S., Catry, F.X., & Oliveira, T.M. (1998). Regional fuel mapping using a knowledge based system approach. *3rd International Conference on Forest Fire Research and 14th Conference on Fire and Forest Meteorology*. 2111 – 2123, Luso, Portugal, November 16 – 20.
- Donovan, G.H., & Rideout, D.B. (2003). An Integer Programming Model to Optimize Resource Allocation for Wildfire Containment. *Forest Science*, 2, 49.
- ENVI, (2003). *Environment for Visualizing Images (ENVI) User's guide*. Research Systems Inc. Version 4.0., Boulder, CO, 645-647 pp.
- Fallowski, M. J., Gessler, P.E., Morgan, P., Hudak, A. T, & Smith A.M.S. (2005). Characterizing and mapping forest fire fuels using Aster imagery and gradient modeling. *Forest Ecology and Management*, 217(2-3), 129-146.
- Finney, M.A. (1994). Modeling the spread and behavior of prescribed natural fires. In J. D. Cohen, J. M. Saveland, and D. D. Wade, (Eds.), *12th conference on fire and forest meteorology*. Bethesda, MD, Society of American Foresters (pp. 138-143). Jekyll Island, Georgia.
- Finney, M.A. (1995). *FARSITE Fire Area Simulator. Version 1.0. User guide and technical documentation*. Missoula, MT, Systems for Environmental Management Report, 47-62 pp.
- Finney, M.A. (1998). *FARSITE: Fire Area Simulator Model development and evaluation*. USDA, Forest Service Research Report RMRS-RP-4. Rocky Mountain Research Station, Ogden, UT, 53-58 pp.
- Green, A.A., Berman, M., Switzer, P., & Craig, M.D. (1988). A transformation for ordering multispectral data in terms of image quality with implications for noise removal: *IEEE Transactions on Geoscience and Remote Sensing*, 26(1), 65-74.
- Griffin, A.M.R., Popescu, C.S., & Zhao, K. (in review). Using LIDAR and normalized difference vegetation index to remotely determine LAI and percent canopy cover.

- Grupe, M. A. (1998). Assessing the applicability of the terrestrial ecosystem survey for FARSITE. Master's Thesis. Albuquerque, New Mexico. University of New Mexico.
- Hodgson, M.E., Jensen, J.R., Tullis, J.A., Riordan, K.D., & Archer, C.M. (2003). Synergistic use of LIDAR and color aerial photography for mapping urban parcel imperviousness. *Photogrammetric Engineering & Remote Sensing*, 69(9), 973-980.
- Jensen, J.R. (1996). *Introductory digital image processing: A remote sensing perspective*. 2nd edition. Upper Saddle River, NJ. Prentice-Hall Inc. 78-81 pp.
- Jensen, J.R. (2005). *Introductory Digital Image Processing: A remote sensing perspective*. 3rd edition. New Jersey, Prentice-Hall Inc. 114-116 pp.
- Justice, C.O., Malingreau, J.P., & Setzer, A.W. (1993). Satellite remote sensing of fires: Potentials and limitations. *Fire in the environment*. 77-88.
- Keane, R.E., Garner, J.L., Schmidt, K.M., Long, D.G., Menakis, J.P., & Finney, M.A. (1998). *Development of the input data layers for the FARSITE fire growth model for the Selway-Bitterroot wilderness complex*. USDA, Forest Service General Technical Report RMRS-GTR-3. 121 pp.
- Keane, R.E., Mincemoyer, S. A., Schmidt, K.M., Long, D. G., Garner, J. L. (2000). Mapping vegetation and fuels for fire management on the Gila National Forest Complex, New Mexico, [CD-ROM]. Gen. Tech. Rep. RMRS-GTR-46-CD. U.S. Department of Agriculture, Forest Service, Rocky Mountain Research Station, Ogden, UT , 126 pp.
- Keuchel, J., Naumann, S., Heiler, M., & Siegmund, A. (2003). Automatic land cover analysis for Tenerife by supervised classification using remotely sensed data. *Remote Sensing of Environment*. 86(4), 530-541.
- Lefsky, M. A., Cohen, W.B., Parker G.G., & Harding D.J. (2002). LIDAR remote sensing for ecosystem studies. *BioScience*, 52, 1,
- Lillesand, T.M., & Kiefer, R.W., (1994). *Remote Sensing and Image interpretation*, 3rd edn. New York ,Wiley , 585-618 pp.
- Llinas, J., (2002). Center for multisource information fusion university at Buffalo, Buffalo, NY. Online at:
<http://www.infofusion.buffalo.edu/tm/Dr.Llinas'sstuff/DataFusionOverview.ppt#1>

- Lunetta, R.S., Congalton, R.G., Fenstermaker, L.K., Jensen, J.R., McGwire, K.C., & Tinney, L.R. (1991). Remote sensing and geographic information system data integration: Error sources and research issues. *Photogrammetric Engineering & Remote Sensing*, 57(6), 677-687.
- Mark, C.A., Bushey, C.L., & Smetanka, W. (1995). *Fuel model identification and mapping for fire behavior prediction in the Absaroka-Beartooth Wilderness, Montana and Wyoming*. Symposium on fire in wilderness and park management. USDA, Forest Service General Technical Report INT-GTR-320. Intermountain Research Station. Logan, UT, 227-229.
- Means, J.E. (2000). Comparison of large-footprint and small-footprint lidar systems: design, capabilities, and uses. *2nd International Conference on Geospatial Information in Agriculture and Forestry*, Lake Buena Vista, Florida, 10-12.
- Miller, J.D., & Yool, S.R. (2000). Modeling fire in semi-desert grassland/oak woodland: the spatial implication. *Ecological Modeling*, 153(3), 229-245.
- Morsdorf, F., Meier, E., Kötz, B., Itten, K.I., Dobbartin, M. & Allgöwer, B. (2004). LIDAR-based geometric reconstruction of boreal type forest stands at single tree level for forest and wild land fire management. *Remote Sensing of Environment*, 92(3), 353-362.
- National Fire and Aviation Management Web Applications. Online at: http://www.fs.fed.us/fire/planning/nist/wims_web_userguide.htm. Accessed on April, 2006.
- Naesset, E., & Okland, T. (2002). Estimating tree height and tree crown properties using airborne scanning laser in a boreal nature reserve. *Remote Sensing of Environment*, 79(1), 105-115.
- Nelson, R., Valenti, M. A., Short, A., & Kelley, C. (2003). A multiple resource inventory of Delaware using airborne laser data. *Bioscience*, 53(10), 981-992.
- Popescu, C.S., & Zhao, K. (in review). LIDAR tomography of forest vegetation: an application for estimating crown base height for deciduous and pine trees.
- Popescu, S.C., Wynne, R. H., & Nelson, R.F. (2003). Measuring individual tree crown diameter with LIDAR and assessing its influence on estimating forest volume and biomass. *Can. J. Remote Sensing*, 29(5), 564-577.
- Popescu, S.C., Wynne, R.H., & Scrivani, J.A. (2004). Fusion of small-footprint lidar and multispectral data to estimate plot-level volume and biomass in deciduous and pine forests in Virginia, U.S.A. *Forest Science*, 50(4), 551 -565 .

- Pyne, S.J., Andrews, P.L., & Laven, P.D. (1996). *Introduction to wildland fire*. New York. Wiley & Sons Press. 22-45 pp.
- Riano, D., Chuvieco, E., Salas, J., Palacios-Orueta, A., & Bastarrika, A. (2002). Generation of fuel type maps from Landsat TM images and ancillary data in Mediterranean ecosystem. *Canadian Journal For Res.*, 32, 1301-1315.
- Riano, D., Meier, E., Allgower, B., Chuvieco, E., & Ustin, S.L. (2003). Modeling airborne laser scanning data for the spatial generation of critical forest parameters in fire behavior modeling. *Remote Sensing of Environment*, 86(2), 177-186.
- Richards, G.D. (1990). An elliptical growth model of forest fire fronts and its numerical solution. *Int. J. Numer. Meth. Eng.*, 30, 1163-1179.
- Reeves, H.C. (1988). *Photo guide for appraising surface fuels in east Texas*. Center for applied studies at School of forestry. Nacogdoches, Texas, Stephen F. Austin State University, 43-51 pp.
- Roberts, D., M. Gardner, J. Regelbrugge, D. Pedreros, & Ustin, S. (1998). Mapping the distribution of wildfire fuels using AVIRIS in the Santa Monica Mountains. Online at: <http://cstars.ucdavis.edu/nasa-essp/smm-fires/paper.html>. 6.
- Roff, A., Goodwin, N., & Merton, R. (2005). *Assessing fuel loads using remote sensing*. School of Biological, Earth & Environmental Science Technical Report summary. The university of New South Wales SYDNEY, NSW 2052 Australia, 11-17 pp.
- Rothermal, R.C. (1972). *A mathematical model for predicting fire spread in wildland fuels*. USDA, Forest Service, Research Paper INT-115. Intermountain Forest and Range Experiment Station. Ogden, UT, 44 pp.
- Scott, J. H., & Reinhardt, E. D. (2001). *Assessing crown fire potential by linking models of surface and crown fire behavior*. USDA, Forest Service Research Paper RMRS-RP-29, Rocky Mountain Research Station, Fort Collins, CO, 9-21 pp.
- Smith, L. I. (2002). A tutorial on principal component analysis. Online at : http://csnet.otago.ac.nz/cosc453/student_tutorials/principal_components.pdf.
- Stephens, S. L. (1997). Evaluation of the effects of silvicultural and fuels treatments on potential fire behavior in Sierra Nevada mixed-conifer forests. *Forest Ecology and Management*, 105, 21-35.

- Stratton, D.R., (2004). Assessing the effectiveness of landscape fuel treatments on fire growth and behavior. *Journal of Forestry*, 32-40
- TFS, (2006). Texas Forst Service. Online at;
<http://texasforests-service.tamu.edu/shared/article.asp?DocumentID=1197>
- Wagner, V., C.E. (1993). Prediction of crown fire behavior in two stands of jack pine. *Can. J. For. Res.*, 23, 442–449.
- Wagner, W., Eberhofer, C., & Summer, G. (2004). Rbust filtering of airborne laser scanning data for vegetation analysis. *International Archivews and Photogrammetry, Remote Sensing and Spatial Information Sciences*. 36(8), 56-61.

VITA

Muge Mutlu received her BAR of Landscape Architecture degree from the Dept. of Landscape Architecture, Cukurova University, Adana, Turkey. She entered the Spatial Science Lab, Dept. of Forest Science at Texas A&M University in 2004 and she received her Master of Science degree in December 2006. She will continue her studies toward a PhD degree in the same department.

Mrs. Mutlu may be reached at Spatial Science Lab, 1500 Research Parkway, Suite B215, College Station, TX. Her e-mail address is mugemutlu@tamu.edu or mugekaan@gmail.com.